Conductance Enhancement of InAs/InP Heterostructure Nanowires by Surface Functionalization with Oligo(phenylene vinylene)s

Muhammed Ihab Schukfeh,[†] Kristian Storm,[‡] Ahmed Mahmoud,[§] Roar R. Søndergaard,[∥] Anna Szwajca,[†,⊥] Allan Hansen,[†] Peter Hinze,[#] Thomas Weimann,[#] Sofia Fahlvik Svensson,[‡] Achyut Bora,[†,§] Kimberly A. Dick,[‡,○] Claes Thelander,[‡] Frederik C. Krebs,[∥] Paolo Lugli,[§] Lars Samuelson,[‡] and Marc Tornow[†,§,*]

[†]Institut für Halbleitertechnik, Technische Universität Braunschweig, Germany, [‡]Solid State Physics/the Nanometer Structure Consortium, Lund University, Sweden, [§]Institute for Nanoelectronics, Technische Universität München, Germany, [∥]Department of Energy Conversion and Storage, Technical University of Denmark, Denmark, [⊥]Faculty of Chemistry, A. Mickiewicz University, Poznan, Poland, [#]Physikalisch-Technische Bundesanstalt, Braunschweig, Germany, and [○]Polymer and Materials Chemistry, Lund University, Sweden

ABSTRACT We have investigated the electronic transport through 3 μm long, 45 nm diameter InAs nanowires comprising a 5 nm long InP segment as electronic barrier. After assembly of 12 nm long oligo(phenylene vinylene) derivative molecules onto these InAs/InP nanowires, we observed a pronounced, nonlinear $I-V$ characteristic with significantly increased currents of up to 1 μA at 1 V bias, for a back-gate voltage of 3 V. As supported by our model calculations based on a nonequilibrium Green Function approach, we attribute this effect to charge transport through those surface-bound molecules, which electrically bridge both InAs regions across the embedded InP barrier.

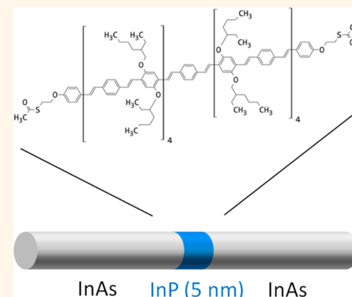

KEYWORDS: nanowires · heterostructure · InAs · molecular electronics · oligo(phenylene vinylene)

The transfer of charges across the interface between organic molecules and semiconductor material is of large significance in various areas of applied research including photovoltaics, sensors and nanoelectronics. Much fundamental work has focused on the detailed understanding of the underlying transport mechanisms, in particular, for organic self-assembled monolayers (SAMs) on silicon-based substrates, here mostly using semiconductor-SAM-metal sandwich architectures.[1−4] When compared to metals, semiconductors offer a much broader range of parameters that can be tailored toward dedicated electronic properties, including band gap, doping type, and concentration, and eventually thin surface dielectrics like oxides. While a large variety of molecular electronic transport studies has been carried out on molecules bridging two metal electrodes,[5−11] only few reports have been published on all-semiconductor contacts.[12−14]

The narrow-band gap semiconductor indium-arsenide (InAs) is a material of particular interest for such applications due to the presence of an electron inversion or accumulation layer at the surface.[15] This is in contrast to most other semiconductors that feature a surface depletion layer. For this reason, a low-resistance, metal-like contact of organic molecules to InAs may be expected once these molecules have formed a chemical bond to the substrate *via*, for example, a terminal thiol group.[16−18] The formation of an InAs contact pair with separation in the few nanometer regime, however, using the common concept of inserting an insulating barrier material between two conductive electrode layers,[19−21] is difficult to achieve. This originates from the fact that in planar, layered heterostructure

* Address correspondence to tornow@tum.de.

Received for review January 24, 2013 and accepted April 23, 2013.

Published online April 30, 2013
10.1021/nn400380g

© 2013 American Chemical Society

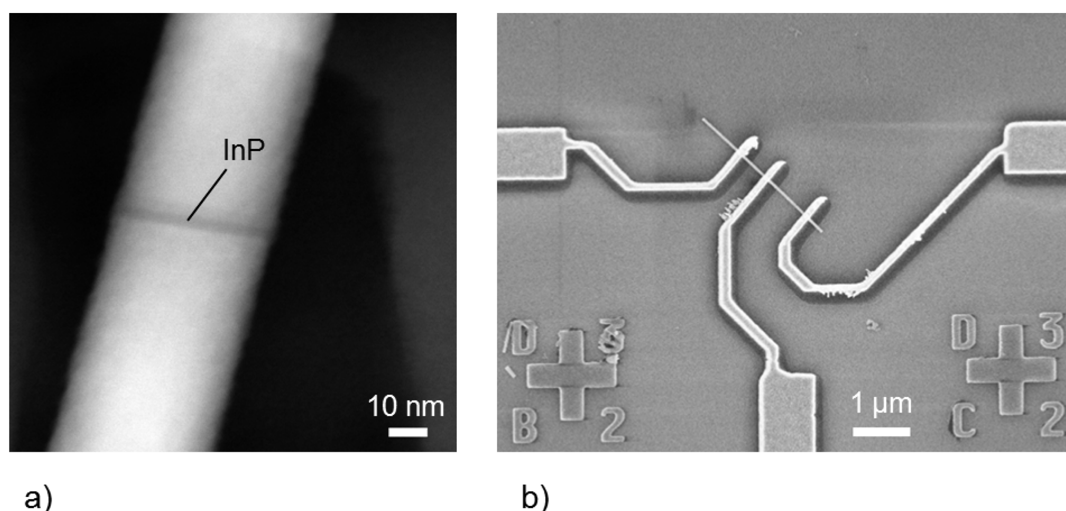

Figure 1. Electron microscopy images of InAs/InP heterostructure nanowires. (a) Scanning transmission electron microscopy (STEM) image of the central region; the embedded InP segment is visible as dark stripe. (b) Scanning electron microscopy (SEM) image of an individual, 2.8 μm long wire contacted by three metal leads as ohmic contacts (Ti/Au 5/100 nm, lateral width *ca.* 200 nm), prepared by electron-beam lithography (EBL). Contacting with three leads allows for the simultaneous measurement of a wire section with InP barrier (between right and center contact) and a wire section without barrier (bare InAs, between left and center contact). Two markers with coordinates for EBL alignment can be seen at the bottom of the image.

growth techniques, such as molecular beam epitaxy, InAs cannot easily be alternated with suitable larger band gap materials such as InP due to the lattice constant mismatch. These obstacles have been overcome by the mature technology of nanowire heterostructure growth,[22] where, for example, InP barriers of almost arbitrary length can be embedded into InAs nanowires during epitaxial growth.[23] Hence, the formation of an InAs nanoscale electrode pair, electronically separated by an InP barrier, could allow for the formation of a novel type of molecular electronic device once suitably functionalized with organic molecular species that would bridge the barrier from InAs to InAs.

In this article, we report on the realization of such a device using InAs nanowires with 5 nm InP barriers that were functionalized with 12 nm long oligo(phenylene vinylene) (OPV) molecular wires. We attribute the observed strong increase of conductance after surface coating to resonant electronic transport through the OPV molecular orbitals.

RESULTS AND DISCUSSION

We have prepared InAs/InP heterostructure nanowires using a vapor–liquid–solid (VLS) growth mode as reported previously.[24] The ~3 μm long InAs wires of typical diameter 45 $\pm$ 4 nm, with growth-induced n-doping, featured an about 5 nm long embedded InP-segment (typically 5 $\pm$ 2 nm), located about 1.5 μm from the top end. Figure 1a shows a scanning transmission electron microscopy (STEM) image of the central part of such a wire comprising the InP segment.

Electrical characterization measurements of individually contacted nanowire samples (*cf.* Figure 1b) were carried out before and after molecular surface

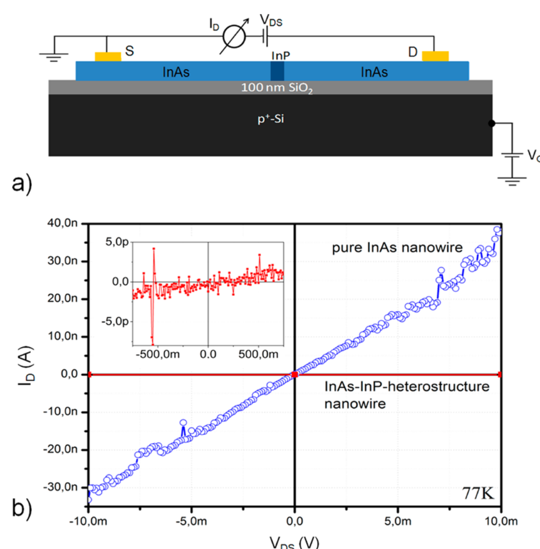

Figure 2. (a) Schematic circuitry setup of the contacted InAs/InP nanowire, on top of an oxide covered p^+-Si substrate acting as backgate. (b) Current–voltage characteristics (at V_G = 0 V) of unfunctionalized reference samples: one pure InAs nanowire (blue open circles and line) and one InAs/InP nanowire (red full circles and line) at 77 K. Data points for the InAs/InP wire were taken in 10 mV steps, the inset shows the I–V trace in a larger range, up to $\pm$750 mV.

functionalization at 77 K, in the dark. Figure 2a shows a schematic of the employed electrical circuitry setup.

Prior to the electrical measurements of heterostructure nanowires functionalized with organic molecules we precharacterized these wires, together with pure InAs wires, to verify proper electrical function. As shown in Figure 2b, a pure InAs wire reveals a linear, ohmic behavior with an overall, typical resistance of some 300 kΩ. Here, the contribution of the Ti/Au ohmic contacts adds to the bare wire resistance. We note that

the $I-V$ trace is linear even around zero bias underlining the good ohmic characteristics of the evaporated metal contacts. The bare InAs wires show a moderate dependence on the applied gate voltage, with a ~25% increase of the low bias conductance between $V_G = 1$ and 3 V at room temperature (Figure S1, Supporting Information). An increase of conductance is expected due to the growing electronic charge density in the InAs surface accumulation layer upon application of a positive gate voltage.

In contrast to the bare InAs wires, the heterostructure wires comprising the 5 nm long InP segment show excellent electrical insulation, with resistances of up to more than 100 GΩ (Figure 2b). This verifies the InP segment acting as barrier to electronic transport. The barrier originates from the energy difference of ~600 meV between the conduction band edges of InAs and InP at the abrupt heterointerface (conduction band offset) .[24]

To test the applicability of our novel, semiconductor nanowire-based contact scheme for molecular conductance studies, we chose 12 nm long OPV derivatives (Figure 3a) that can be surface-assembled from solution. The molecules with π-conjugated backbone were synthesized as described previously.[25] The OPVs were end-terminated by two thioacetyl groups (connected by short $[CH_2]_2$-O- linkers), to provide the tethering to the InAs, by forming surface-bound thiolates presumably to the indium.[17,26,27] Prior to functionalization of the InAs/InP wires, we investigated the molecule deposition on a planar InAs surface by atomic force microscopy (AFM) imaging and nanolithography techniques. A 5 × 5 μm^2 surface was first scanned in tapping mode. Then, a 1 × 1 μm^2 square within the prescanned area was "scratched" free of molecules by using contact mode, effectively moving the molecules to the square edges. Finally, the initial scanning area was measured again in tapping mode, imaging the exposed, free InAs square, see, Figure 3b. Averaged line scans (height profiles) allowed for a measurement of the molecular layer thickness with respect to the clean InAs surface, as displayed in the inset of Figure 3b.

A layer thickness of ~2.2 ± 0.4 nm was obtained from this analysis. We also measured the thickness by ellipsometry, which yielded a slightly larger value of 2.8 ± 0.2 nm. This small discrepancy may arise from local surface roughness (bright spots in AFM image, Figure 3b) that were not taken into account for AFM height profiling. Clearly, these thickness values would not indicate the formation of a self-assembled monolayer (SAM) with upright-standing molecules. Rather, it appears more likely that molecules which have potentially bound with one or both ends to the substrate would lie down. The lateral width of the OPV derivative measures about 2.2 nm, including the branched side chains. Hence, a compact layer of lying,

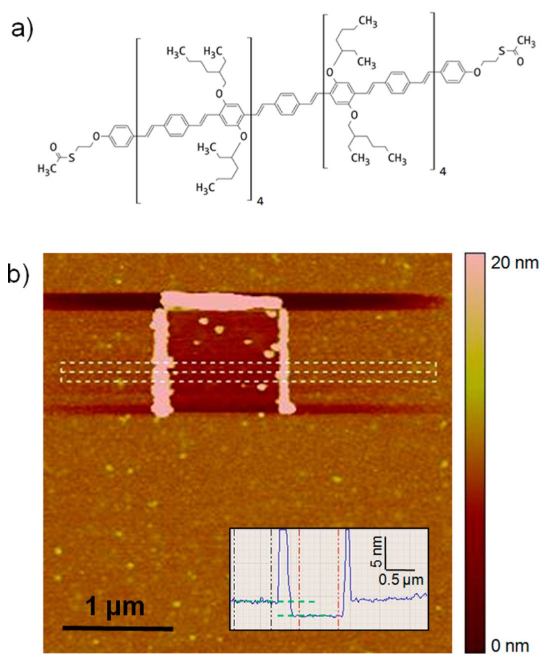

Figure 3. (a) Structural formula of the investigated OPV derivative molecule. (b) AFM image of an InAs surface after deposition of the molecule shown in (a). A 1 × 1 μm^2 square was scratched free from molecules, which have visibly piled up at the edges of the square. The dark horizontal bars extending from these regions are imaging artifacts. A height profile line scan, averaged over the area within the white dashed line box, is shown in the inset. Averaging between the red and black cursor lines, respectively, yields a step height of 2.2 ± 0.4 nm.

possibly laterally stacked molecules may explain our finding. To support our conclusion that the molecules were chemically grafted to the surface by thiolate bonds, we conducted a control experiment with a structural analog of the OPV, which however featured −OH groups instead of the thioacetyl groups linked to the terminal phenyls. Very little surface coating could be detected in this case (order of 0.5 nm thickness), most likely due to mere physisorption with the OPVs lying flat on the surface (Figure S4, Supporting Information). Hence, we conclude that in contrast the thiolate terminated OPVs have formed a chemisorbed, compact monolayer of lying molecules on the surface of planar InAs.

Following the same procedure for molecule deposition as was used for the planar InAs surfaces we coated the InAs/InP heterostructure nanowires that had been electrically precharacterized, using the original OPV derivative shown in Figure 3a. Only those nanowires were chosen for this step that had shown highly insulating characteristics before. The $I-V$ characteristic of one such unfunctionalized heterostructure wire with currents below 200 pA between +3 V and −2 V, measured at T = 77 K, is included in Figure 4. The observed increase of current at more negative voltages might be due to (soft) dielectric breakdown of the InP segment. After warming the sample back to room

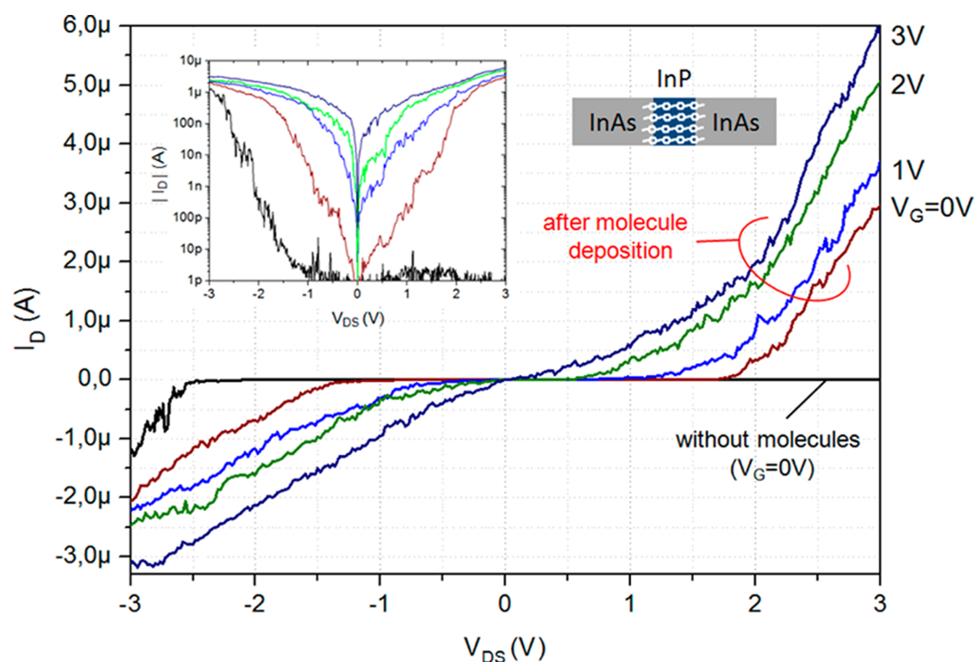

Figure 4. ***I*–*V* traces of an InAs/InP nanowire before and after surface functionalization with OPV derivatives, as function of back-gate voltage, measured at 77 K. Left inset: same *I*–*V* traces in a semilogarithmic plot, for the absolute value of I_D as function of V_{DS} (same color coding). Right inset: schematic illustration of how OPV molecules may electrically bridge the InP barrier segment.**

temperature, the nanowire was surface-coated with molecules and cooled again to 77 K. Figure 4 summarizes the *I*–*V* characteristics of the same nanowire measured before as reference, now functionalized, and as function of back-gate voltage. Clearly, the current has significantly increased for the entire bias range after functionalization, partly up to more than 6 orders of magnitude, while still keeping V_G = 0 V (inset in Figure 4). In total, we have observed a qualitatively similar increase of conductance for OPV coated InAs/InP nanowires in three individual experiments (see Figure S2, Supporting Information).[28,29] In the linear current scaling of Figure 4, the prominent conductance gap now appears significantly reduced with respect to the clean wire, ranging from about −1.5 to 1.5 V. From these voltages on, the drain current I_D enhances up to a few μA at ±3 V. When a positive backgate voltage is applied, the threshold for this significant onset of conductance shifts rapidly to smaller source-drain bias, turning the ∼3 V wide conductance gap observed at V_G = 0 V to a zero width one for V_G = 3 V, with approximately linear *I*–*V* and a resistance of about 1–2 MΩ at small bias.

We attribute the observed, strong impact of OPV functionalization on the nanowire conductance to electronic transport through the surface assembled molecular wires which may have directly bridged the embedded InP segment, thereby connecting both InAs sides. In general, a change of nanowire electrical properties may also be induced by mere surface passivation with thiols.[17,30] To exclude such chemisorption effects on the conductance of our nanowires we carried out control experiments with InAs wires having a 7 ± 2 nm InP barrier. We functionalized these wires with a ∼5 nm long OPV analog derivative, featuring the same terminal binding groups as for the 12 nm OPV shown in Figure 3a. The assembly was verified on a planar InAs substrate, with measured ellipsometric thickness 2.7 ± 0.1 nm. We did not observe any increase in conductance of the InAs/InP wire after functionalization, independent of gate voltage (Supporting Information, Figure S3). We ascribe this finding to the fact that (1) the mere surface thiolate bond formation alone did not enhance the junction conductance and that (2) these molecules were too short to bridge the InP barrier electrically, as expected.

N-type InAs comprises an electron surface accumulation layer providing a 2D metallic type of conductance which is also reflected in the *I*–*V* trace displayed in Figure 2b. In our heterostructure nanowires the conduction band offset between InAs and InP introduces a 600 meV electronic barrier of 5 nm length for electrons that are to traverse the InP segment. This barrier suppresses the conductance considerably. A possible conduction path could be tunneling through the barrier. Based on the Simmons model,[31] we estimate a small bias resistance of about 60 MΩ at 100 mV for nonresonant tunneling only (see Supporting Information). The currents at 100 mV for both the functionalized and the reference heterostructure wire, however, were measured to be even more than 2 orders of magnitude lower than expected from this estimate.

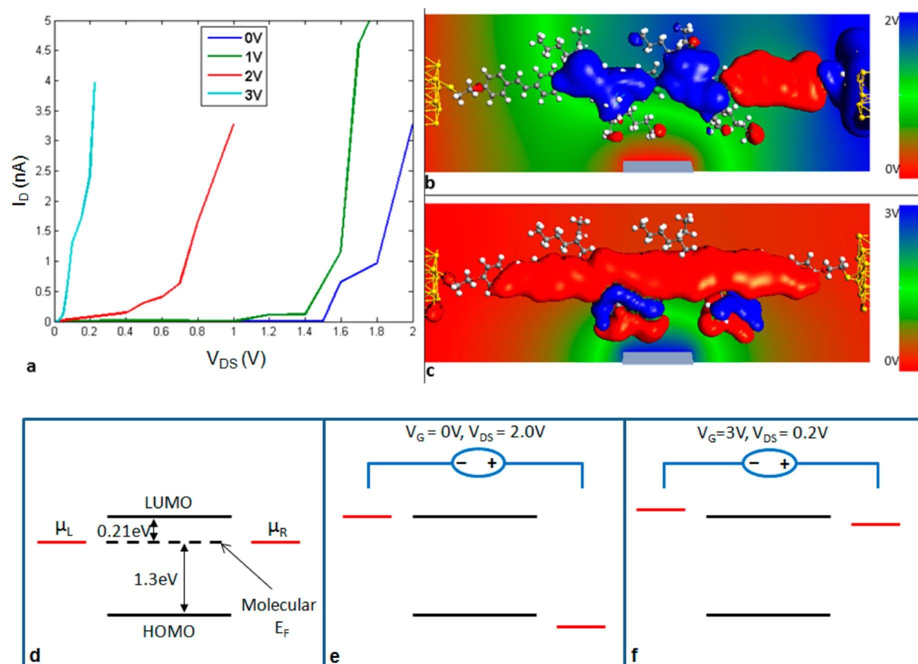

Figure 5. (a) Calculated current–voltage characteristics for various gate voltages. (b) Total charge density of the resonant orbital for V_G = 0 V, V_{DS} = 2 V and (c) for V_G = 3 V, V_{DS} = 0.2 V. (d–f) Schematic energy diagrams at equilibrium, at V_G = 0 V and V_{DS} = 2.0 V, and at V_G = 3 V and V_{DS} = 0.2 V, respectively. μ_L and μ_R are the chemical potentials of the left and right electrode, respectively. Energy diagrams are qualitative and not drawn to scale. See Figures S5 and S6 (Supporting Information) for the quantitative transmission spectra.

While the measured low conductance persists up to a few volts bias for the unfunctionalized InAs/InP reference wire, the same wire reveals a significant current enhancement after molecule assembly above a certain threshold voltage, as described above. From the molecule geometry and size and from our finding for the assembly on planar surfaces, we estimate a maximum total number of about 300 OPVs that may align in parallel around the circumference of the wire, thereby eventually bridging the InP region (schematic sketch in Figure 4). In our previous experiments investigating the same molecule connected to about 9 nm separated Au electrodes, we observed the same qualitative current–voltage behavior, with the same typical threshold voltage for the onset of conductance, without applied gate voltage.[25,32] We note, however, that the absolute magnitude of currents reached in our present work is by orders of magnitude larger, even for a possibly smaller number of molecules. This may well result from the smaller barrier length that could allow partial charge transfer directly into the conjugated backbone of the OPV or from the proximity of the InP barrier material that may also affect the molecular orbital energetic landscape.

In general, different electronic transport paths through the molecule may contribute. While the inner part of the molecule comprises a conjugated electron system, the short alkyl-oxygen linker groups at the termini of the OPV effectively decouple it from the contacts, acting as electronic barriers of height ~1 eV. We note that, without such linker groups, we had observed a much smaller threshold voltage of about 300 mV for similar OPV derivatives, as reported in earlier work.[33] For the present system in general, either Coulomb blockade effects[34] or the transition from nonresonant tunneling to direct, resonant charge transfer through molecular orbital levels may arise.[35] We attribute our observations to the latter mechanism as supported by our model calculations. For this purpose, we rely on our previous calculation of an OPV molecule linked to gold electrodes.[25] There, a conductance gap (approximately −1.5 to 1.5 V, with no gate present) had been observed when a relatively short OPV was linked to Au nanogap contacts. With the help of a density functional theory (DFT) approach coupled to nonequilibrium Green's function (NEGF) methods (Atomistix ToolKit version 11.2.3, QuantumWise A/S, www.quantumwise.com), the transport mechanism responsible for conduction could be qualitatively explained. At low bias, a current is only possible *via* electron tunneling across the OPV HOMO–LUMO gap. Because such a process has a low probability, the corresponding current is negligible. The threshold at 1.5 V corresponds to the bias at which the LUMO (or the HOMO) level becomes aligned with one of the contact Fermi levels, thus, giving the possibility for electrons to go across such a resonance state, with a much lower overall resistance. We have extended the calculation by including a gate electrode located a few nm from the molecule. Extended Hückel theory coupled to the NEGF is employed in the calculation of the gated OPV device.

At zero gate voltage (blue curve in Figure 5a), the previous results are reproduced. Interestingly, when a positive bias is applied to the gate, the threshold voltage decreases, in agreement with the experimental observations, showing basically no threshold behavior already at $V_G = 2$ V (Figure 5a). By looking at the orbital configuration for different gate voltages and at the corresponding energy-dependent transmission probabilities (Figure 5b,c, and Supporting Information, Figures S5 and S6) we can attribute the gate behavior to an electrostatically induced change of the orbitals providing the resonant conductive channels. The positive gate potential attracts electrons to the OPVs and makes the LUMO level available for conductance at a much lower bias than in the absence of the gate, see the schematic energy diagram in Figure 5f. This is reflected by the predominantly negative charge density (depicted with red color, in Figure 5b,c) found on the LUMO at $V_G = 3$ V, $V_{DS} = 0.2$ V, compared to the situation at zero gate voltage ($V_{DS} = 2$ V) where the HOMO level contributes mostly to the conduction. The background color in the two figures reflects the potential profile along the molecule. As mentioned above, the linker groups at the two contacts create a potential barrier between Au and OPV. Each barrier originates due to a charge dipole which in turn is created by the electron charge attracted by the strongly electronegative oxygen atom. At $V_G = 0$, $V_{DS} = 2$ V, most of the potential drop occurs near the linker groups. The application of a positive gate voltage screens both dipoles inducing a more linear potential drop over the whole OPV and the onset of conduction at very small voltages.

Although the calculation refers to a highly simplified system with respect to the experiment (shorter OPV, Au electrodes, and gate electrode in vacuum at short distance from the molecule) we believe that our results can provide a proper picture of the critical processes involved in molecular transport. In particular, we have also calculated the potential distribution in the exact back-gate configuration shown in Figure 2a, using a 3D Poisson solver. The actual potential at the surface of the wire where the OPV molecules are located is around 0.2 eV for $V_G = 3$ V. This is fully consistent with the potential that the molecules experience in the gate configuration we used to calculate the charge transport properties of OPV (Figure 5).

CONCLUSION

We have demonstrated a novel molecular electronics device configuration where the electrical contacts to the organic molecules consist of all-semiconductor material. InAs nanowires comprising a 5 nm embedded InP barrier segment were surface functionalized with 12 nm long OPV derivatives. These OPVs formed a dense layer on planar InAs of thickness ~2.2 nm, as verified by AFM studies. The observed nonlinear $I-V$ characteristics of coated InAs/InP heterostructure nanowires can be understood in terms of electronic transport through those molecules which bridge both InAs halves of the wire across the InP barrier. We attribute the onset of conductance at bias above 1.5 V to resonant tunneling predominantly through the HOMO level of the OPV. This threshold effectively shifts to smaller values with increasing backgate voltage eventually leading to finite, ohmic-like conductance at zero bias, in agreement of experiment and model calculations. Future work shall address to more detail the transport mechanism in our InAs−molecule−InAs system, in particular, taking into account the coupling to the contacts and the influence of the InP dielectric barrier material onto the molecular orbital energetics.

METHODS

InAs/InP Nanowire Sample Preparation. Nanowires were mechanically transferred from the growth sample onto thermally oxidized (100 nm SiO_2), p-doped (Boron, 0.01−0.02 Ω·cm), 9 × 9 mm^2 silicon samples. These Si/SiO_2 samples featured arrays of Pd−Au markers on the surface, prepared by EBL, electron-beam evaporation and lift-off, for assigning coordinates (mapping) to those individual wires to be electrically contacted. Subsequent to transfer, preinspection, selection, and mapping in SEM, we chemically etched the deposited nanowires in a solution of acetic acid and hydrobromic acid (17:3 mL) for 2.5 min at a temperature of 22 °C. This treatment slightly recess-etched the surface of the InP segment, thereby further smoothening/leveling out the heterointerface region. We typically chose 12 nanowires per sample to be electrically contacted, either nine of which contain an InP segment, and three pure InAs wires as reference, or as combined wires shown in Figure 1b. Ohmic contacts to the chosen nanowires together with the metallic leads to larger bond pads at the outer edge of the sample were prepared by EBL using a 560 nm PMMA layer, electron-beam evaporation of 5 nm Ti/100 nm Au and lift-off (Aceton 80 °C, 3 h, rinsing in iso-propanol and deionized water, drying in stream of nitrogen). Subsequently, possible residues of PMMA were removed in O_2 plasma, 30 s. To improve the quality of the ohmic contacts to the InAs wires, their native surface oxide layer was removed and the surface was passivated just before evaporation (transfer time below 2 min) using a dedicated ammonium polysulfide process.[36] After preparation of the ohmic contacts the backside of the sample was etched in a 6% buffered HF solution for 2 min to remove the 100 nm backside oxide. The sample was then mounted in a ceramic chip carrier using melted indium as conductive adhesive. Finally, the front side outer bond pads of the sample were Au wire bonded.

InAs Surface Functionalization with OPV Derivative Molecules. For functionalization studies on planar InAs (100) oriented, centimeter-sized samples (undoped, Wafertech) were at first exposed to buffered HF solution (6%) vapor for 60 s. Right afterward, the samples were immersed in a 72 μM solution of the OPV derivative molecules dissolved in tetrahydrofuran (THF, ≥99.9%) for 24 h. During this time, the solution with sample was kept inside a closed beaker with THF-saturated atmosphere, to avoid concentration changes by evaporation. Subsequent to molecular deposition, the samples were first annealed (60 °C for 1 h, in nitrogen atmosphere), and then kept in isopropanol at 30 °C for 1 h. For acetyl deprotection and thiolate bond activation, the substrates were immersed in a

0.06 M solution of NH_4OH in THF/isopropanol (1:2 w/w) for 1 h. Following this step, the samples were rinsed in THF/iso-propanol and finally blown dry in a stream of nitrogen.

The same recipe was used for surface functionalization of the heterostructure nanowire samples.

AFM and Ellipsometry. AFM imaging and nanolithography was performed using a Veeco Dimension V instrument, equipped with a Nanoscope V controller, and using aluminum-coated silicon tips. For ellipsometry studies, an EL X-02C rotating-analyzer ellipsometer model (DRE Dr. Riss, Ratzeburg) was used, at fixed wavelength λ = 632.8 nm, and angle of incidence 70°, assuming a refractive index of n = 1.55[25] for the organic layer.

Electrical Measurements. A bonded sample chip under study was mounted into a custom-made, shielded measurement rod and immersed into liquid nitrogen. Measurements were taken at 77 K to avoid possible thermionic excitation over the barrier, which had been observed at room temperature previously.[23] Current−voltage ($I-V$) characteristics were taken using a Keithley 2635 source meter connected to source and drain contacts and controlled *via* a PC (LabView software). A variable backgate voltage V_G was applied to the p-doped Si substrate wafer (Agilent E3641A voltage source), with the 100 nm thermal oxide below the nanowire acting as gate insulator. During the measurement of a given nanowire, all electrical contacts connecting further nanowires were set to common ground potential, for protection against damage from possible electrostatic discharge.

Conflict of Interest: The authors declare no competing financial interest.

Acknowledgment. This work was partially financed by the BMBF under Grants 03N8713 and 03X5513 (Junior Research Group "Nanotechnology") and partly by the Fujitsu Laboratories of Europe. The work was also supported by grants from the Swedish Research Council (VR), the Swedish Foundation for Strategic Research (SSF), and the Knut and Alice Wallenberg Foundation (KAW). We gratefully acknowledge M. Schilling and F. Ludwig for granting access to SEM analysis and S. M. Luber for his contributions in an early stage of this work. We thank A. Schmidt, D. Rümmler, and M. Karsten for technological support, V. Bandalo for help with TEM membrane preparation, and C. Bork for help with surface functionalization.

Supporting Information Available: Additional $I-V$ data (Figures S1−3), AFM analysis data (S4), estimation of tunneling current, and calculated transmission curves (S5, S6). This material is available free of charge *via* the Internet at http://pubs.acs.org.

REFERENCES AND NOTES

1. Vilan, A.; Yaffe, O.; Biller, A.; Salomon, A.; Kahn, A.; Cahen, D. Molecules on Si: Electronics with Chemistry. *Adv. Mater.* **2010**, *22*, 140–159.
2. Wang, W.; Scott, A.; Gergel-Hackett, N.; Hacker, C. A.; Janes, D. B.; Richter, C. A. Probing Molecules in Integrated Silicon−Molecule−Metal Junctions by Inelastic Tunneling Spectroscopy. *Nano Lett.* **2008**, *8*, 478–484.
3. Aswal, D. K.; Lenfant, S.; Guerin, D.; Yakhmi, J. V.; Vuillaume, D. Self Assembled Monolayers on Silicon for Molecular Electronics. *Anal. Chim. Acta* **2006**, *568*, 84–108.
4. DiBenedetto, S. A.; Facchetti, A.; Ratner, M. A.; Marks, T. J. Molecular Self-Assembled Monolayers and Multilayers for Organic and Unconventional Inorganic Thin-Film Transistor Applications. *Adv. Mater.* **2009**, *21*, 1407–1433.
5. Akkerman, H. B.; De Boer, B. Electrical Conduction through Single Molecules and Self-Assembled Monolayers. *J. Phys.: Condens. Matter* **2008**, *20*, 013001.
6. Joachim, C.; Ratner, M. A. Molecular Electronics: Some Views on Transport Junctions and Beyond. *Proc. Natl. Acad. Sci. U.S.A.* **2005**, *102*, 8801–8808.
7. Moth-Poulsen, K.; Björnholm, T. Molecular Electronics with Single Molecules in Solid-State Devices. *Nat. Nanotechnol.* **2009**, *4*, 551–556.
8. Reed, M. A.; Lee, T., *Molecular Electronics*; American Scientific Publishers: Los Angeles, CA, 2003.
9. Tao, N. J. Electron Transport in Molecular Junctions. *Nat. Nanotechnol.* **2006**, *1*, 173–181.
10. Cuevas, J. C.; Scheer, E. *Molecular Electronics: An Introduction to Theory and Experiment*; World Scientific: Singapore, 2010.
11. Cai, L. T.; Skulason, H.; Kushmerick, J. G.; Pollack, S. K.; Naciri, J.; Shashidhar, R.; Allara, D. L.; Mallouk, T. E.; Mayer, T. S. Nanowire-Based Molecular Monolayer Junctions: Synthesis, Assembly, and Electrical Characterization. *J. Phys. Chem. B* **2004**, *108*, 2827–2832.
12. Ashwell, G. J.; Phillips, L. J.; Robinson, B. J.; Urasinska-Wojcik, B.; Lambert, C. J.; Grace, I. M.; Bryce, M. R.; Jitchati, R.; Tavasli, M.; Cox, T. I.; Sage, I. C.; Tuffin, R. P.; Ray, S. Molecular Bridging of Silicon Nanogaps. *ACS Nano* **2010**, *4*, 7401–7406.
13. Corley, D. A.; He, T.; Tour, J. M. Two-Terminal Molecular Memories from Solution-Deposited C60 Films in Vertical Silicon Nanogaps. *ACS Nano* **2010**, *4*, 1879–1888.
14. Bof Bufon, C. C.; Arias Espinoza, J. D.; Thurmer, D. J.; Bauer, M.; Deneke, C.; Zschieschang, U.; Klauk, H.; Schmidt, O. G. Hybrid Organic/Inorganic Molecular Heterojunctions Based on Strained Nanomembranes. *Nano Lett.* **2011**, *11*, 3727–3733.
15. Olsson, L. Ö.; Andersson, C. B. M.; Håkansson, M. C.; Kanski, J.; Ilver, L.; Karlsson, U. O. Charge Accumulation at InAs Surfaces. *Phys. Rev. Lett.* **1996**, *76*, 3626–3629.
16. Stine, R.; Petrovykh, D. Y. Oriented Self-Assembled Monolayers of Bifunctional Molecules on InAs. *J. Electron Spectrosc. Relat. Phenom.* **2009**, *172*, 42–46.
17. Hang, Q.; Wang, F.; Carpenter, P. D.; Zemlyanov, D.; Zakharov, D.; Stach, E. A.; Buhro, W. E.; Janes, D. B. Role of Molecular Surface Passivation in Electrical Transport Properties of InAs Nanowires. *Nano Lett.* **2008**, *8*, 49–55.
18. Tanzer, T. A.; Bohn, P. W.; Roshchin, I. V.; Greene, L. H.; Klem, J. F. Near-Surface Electronic Structure on InAs(100) Modified with Self-Assembled Monolayers of Alkanethiols. *Appl. Phys. Lett.* **1999**, *75*, 2794–2796.
19. Tyagi, P. Multilayer Edge Molecular Electronics Devices: A Review. *J. Mater. Chem.* **2011**, *21*, 4733–4742.
20. Li, T.; Hu, W.; Zhu, D. Nanogap Electrodes. *Adv. Mater.* **2010**, *22*, 286–300.
21. Prokopuk, N.; Son, K.-A. Alligator Clips to Molecular Dimensions. *J. Phys.: Condens. Matter* **2008**, *37*, 374116.
22. Lieber, C. M.; Wang, Z. L. Functional Nanowires. *MRS Bull.* **2007**, *32*, 99–108.
23. Björk, M. T.; Ohlsson, B. J.; Sass, T.; Persson, A. I.; Thelander, C.; Magnusson, M. H.; Deppert, K.; Wallenberg, L. R.; Samuelson, L. One-Dimensional Steeplechase for Electrons Realized. *Nano Lett.* **2002**, *2*, 87–89.
24. Björk, M. T.; Ohlsson, B. J.; Thelander, C.; Persson, A. I.; Deppert, K.; Wallenberg, L. R.; Samuelson, L. Nanowire Resonant Tunneling Diodes. *Appl. Phys. Lett.* **2002**, *81*, 4458–4460.
25. Søndergaard, R.; Strobel, S.; Bundgaard, E.; Norrman, K.; Hansen, A. G.; Csaba, G.; Lugli, P.; Tornow, M.; Krebs, F. C. Conjugated 12 nm Long Oligomers as Molecular Wires in Nanoelectronics. *J. Mater. Chem.* **2009**, *19*, 3899.
26. Petrovykh, D. Y.; Yang, M. J.; Whitman, L. J. Chemical and Electronic Properties of Sulfur-Passivated InAs Surfaces. *Surf. Sci.* **2003**, *523* (3), 231−240.
27. Knoben, W.; Brongersma, S. H.; Crego-Calama, M. Preparation and Characterization of Octadecanethiol Self-Assembled Monolayers on Indium Arsenide (100). *J. Phys. Chem. C* **2009**, *113*, 18331–18340.
28. A total of 19 initially insulating InAs/InP wires were tested. A total of 15 of these were found destroyed in SEM inspection after the complete series of experiments, probably due to electrostatic discharge or mechanical stress upon thermal cycling. The data of three functional wires are presented; one wire remained insulating.
29. At the same bias of $V_{DS} = -1.5$ V (zero gate voltage) we measured for device 1 an increase of current by about 4 orders of magnitude, for device 2 by almost 4 orders of magnitude, and for device 3 by 1−2 orders of magnitude, respectively.

30. Schvartzman, M.; Sidorov, V.; Ritter, D.; Paz, Y. Passivation of InP Surfaces of Electronic Devices by Organothiolated Self-Assembled Monolayers. *J. Vac. Sci. Technol., B: Microelectron. Process. Phenom.* **2003**, *21*, 148–155.
31. Simmons, J. G. Generalized Formula for the Electric Tunnel Effect between Similar Electrodes Separated by a Thin Insulating Film. *J. Appl. Phys.* **1963**, *34*, 1793–1803.
32. Our used vertical nanogap electrodes based on silicon-on-insulator substrates did not have an integrated gate electrode.
33. Luber, S. M.; Zhang, F.; Lingitz, S.; Hansen, A. G.; Scheliga, F.; Thorn-Csanyi, E.; Bichler, M.; Tornow, M. High-Aspect-Ratio Nanogap Electrodes for Averaging Molecular Conductance Measurements. *Small* **2007**, *3*, 285–289.
34. Danilov, A.; Kubatkin, S.; Kafanov, S.; Hedegård, P.; Stuhr-Hansen, N.; Moth-Poulsen, K.; Bjørnholm, T. Electronic Transport in Single Molecule Junctions: Control of the Molecule-Electrode Coupling Through Intramolecular Tunneling Barriers. *Nano Lett.* **2008**, *8*, 1–5.
35. Song, H.; Kim, Y.; Jang, Y. H.; Jeong, H.; Reed, M. A.; Lee, T. Observation of Molecular Orbital Gating. *Nature* **2009**, *462*, 1039–1043.
36. Suyatin, D. B.; Thelander, C.; Björk, M. T.; Maximov, I.; Samuelson, L. Sulfur Passivation for Ohmic Contact Formation to InAs Nanowires. *Nanotechnology* **2007**, *18*, 105307.